Journal of Sound and Vibration 332 (2013) 5543–5558

Contents lists available at SciVerse ScienceDirect

Journal of Sound and Vibration

journal homepage: www.elsevier.com/locate/jsvi

An energy-preserving description of nonlinear beam vibrations in modal coordinates

Andrew Wynn [a], Yinan Wang [a], Rafael Palacios [a,*], Paul J. Goulart [b]

[a] Department of Aeronautics, Imperial College, London SW7 2AZ, United Kingdom
[b] Automatic Control Laboratory, Swiss Federal Institute of Technology (ETH), 8092 Zurich, Switzerland

ARTICLE INFO

Article history:
Received 25 February 2013
Accepted 7 May 2013
Handling Editor: L.N. Virgin
Available online 2 July 2013

ABSTRACT

Conserved quantities are identified in the equations describing large-amplitude free vibrations of beams projected onto their linear normal modes. This is achieved by writing the geometrically exact equations of motion in their intrinsic, or Hamiltonian, form before the modal transformation. For nonlinear free vibrations about a zero-force equilibrium, it is shown that the finite-dimensional equations of motion in modal coordinates are energy preserving, even though they only approximate the total energy of the infinite-dimensional system. For beams with constant follower forces, energy-like conserved quantities are also obtained in the finite-dimensional equations of motion via Casimir functions. The duality between space and time variables in the intrinsic description is finally carried over to the definition of a conserved quantity in space, which is identified as the local cross-sectional power. Numerical examples are used to illustrate the main results.

1. Introduction

Conserved quantities in nonlinear Hamiltonian systems provide useful metrics to derive numerical integration algorithms, to evaluate their stability, and to derive energy-based controllers. For geometrically nonlinear beams, energy- and moment-preserving time-marching algorithms were first identified in the groundbreaking work of Simó et al. [1,2]. Their approach, later refined by many others [3–5], can be summarized as follows: the partial differential equations of motion are first written for the position and orientation of the beam cross sections, a time-marching algorithm on those variables is then identified that preserves exactly the conservation of laws of the continuum problem, and a finite-element discretization is finally introduced on the weak form of the equations that inherits those same conservation properties. The main challenge was posed by handling both the updating and spatial interpolation of the (finite) rotations and it was overcome using the properties of the rotation group. Robust finite-element solutions for flexible multibody dynamics have been constructed based on this approach (see, for instance, Ref. [6]).

The above methodology does not extend however to nonlinear beam dynamics written in modal coordinates. In such a case, the spatial projection would need to be introduced first, but the infinite-degree nonlinearities associated to the rotation group would need to be truncated before they could be projected onto modal space. This was done, for instance, in Refs. [7,8]. Even so, a solution of the nonlinear problem using modal coordinates is often attractive. For example, there are many dynamical systems with weak nonlinearities for which linear modal vibration analysis provides a useful first approximation to the response, and for which those modal coordinates may suit naturally a more refined subsequent

* Correspondence to: Room 355, Roderic Hill Building, South Kensington Campus. Tel.: +44 20 7594 5075.
E-mail addresses: r.palacios-nieto@imperial.ac.uk, rpalacio@imperial.ac.uk (R. Palacios).

0022-460X
http://dx.doi.org/10.1016/j.jsv.2013.05.021

Nomenclature

$\mathbf{C}$	cross-sectional flexibility matrix
$\mathcal{C}$	Casimir function
$\mathbf{e}_1$	unit vector in the beam axial direction
$\mathcal{E}_0(\mathbf{x}_1,\mathbf{x}_2)$	total energy
$\mathcal{E}_{\overline{\mathbf{x}}_2}(\delta\mathbf{x}_1,\delta\mathbf{x}_2)$	perturbation energy
$\mathcal{E}^N_{\overline{x}_2}(\mathbf{q}_1,\mathbf{q}_2)$	perturbation energy of discrete system
$\mathbf{f}$	vector of sectional internal forces (stress resultants)
$\mathbf{f}_1$	vector of applied forces and moments per unit length
$\mathbf{f}_a$	vector of applied forces per unit length
I_T	average cross-sectional power
$\mathbf{k}_0$	local initial curvature vector
L	symmetric differentiation operator
$\mathcal{L}_1,\mathcal{L}_2$	matrix operators in nonlinear equilibrium equations
$\mathbf{m}$	vector of sectional internal moments (stress resultants)
$\mathbf{m}_a$	vector of applied moments per unit length
$\mathbf{M}$	cross-sectional mass matrix
q_{1j}	modal coordinates (velocities) of mode j
q_{2j}	modal coordinates (internal forces/moments) of mode j
s	curvilinear coordinate (arc length)
S	total beam span
t	time
$\mathbf{v}$	vector of local translational velocities
$V(\mathbf{q})$	Lyapunov function
W	linear dynamics of the unforced ODE system
$\mathbf{x}_1$	velocity states in the intrinsic model
$\mathbf{x}_2$	stress-resultant states in the intrinsic model
$\overline{\mathbf{x}}_2$	equilibrium condition under constant forcing ODE
η_{1j}	generalized force corresponding to mode j
ϕ_j	mode shape of linear normal mode j
$\boldsymbol{\omega}$	vector of local angular velocities
ω_j	angular frequency of linear normal mode j
$\boldsymbol{\Omega}$	diagonal matrix of angular frequencies
$\mathrm{lcm}(T_1,T_2)$	least common multiple of $T_1,T_2\in\mathbb{R}$
$\overline{\bullet}$	value at static equilibrium conditions

nonlinear analysis (see, for instance, many of the examples in Ref. [9]). Additionally, most methods for nonlinear vibration control still rely on modal coordinates to provide a compact low-order representation of the system dynamics [8,10].

In this context, Palacios [11] has recently shown that an exact modal representation of the geometrically nonlinear beam dynamics, with only quadratic nonlinearities, is actually possible if the equations of motion are first written in their intrinsic form [12,13]. This approach uses a two-field description of the beam dynamics on first derivatives, both in space and time, resulting in a model in which the primary variables are stress resultants and local velocities, respectively. Rotations therefore do not appear explicitly in the equations of motion. Instead, they are obtained as either spatial or time integrals of the local curvatures or angular velocities, respectively. The resulting Hamiltonian formulation closely resembles that of rigid-body dynamics, with first-order equations of motion and quadratic nonlinearities. Energy-based control methods developed for Hamiltonian systems [14] can then be applied to nonlinear vibration control. Although limited to linear vibrations, Macchelli and Melchiorri [15] have already successfully shown the use of energy shaping methods in the vibration reduction on beams when their dynamics are written in intrinsic form.

Direct solution of the (nonlinear) intrinsic beam equations of motions has been carried out for aeroelastic analysis of high-aspect-ratio-wing aircraft, using aerodynamic models which only depend on the local velocities [16–18]. The major drawback of such an approach is that multipoint constraints in displacements cannot be imposed directly on the system states. Numerical integration methods can then be borrowed from multibody dynamics, although effective numerical methods have been developed recently specifically tailored to this problem [19]. The modal projection of the equations, on the other hand, uses the linear normal modes (LNMs) of the structure, albeit expressed in terms of the intrinsic degrees of freedom. However, those *intrinsic* LNMs do correspond to the vibration modes of a linearized displacement-based model and can be obtained from them by simply taking derivatives with respect to time and space [20]. Seen in this light, the intrinsic formulation becomes simply an artifice to describe the nonlinear beam dynamics without having to include the rotation vector in the equations. Palacios [11] used this to show substantial algebraic advantages in the evaluation of the nonlinear normal modes of anisotropic beams using the method of Pierre and Shaw [21].

This paper presents a theoretical investigation into the conservation laws in the intrinsic modal description of the nonlinear beam dynamics. As mentioned above, this is relevant when developing methods for nonlinear vibration control, but also to identify relevant metrics to evaluate the performance of time-marching algorithms in nonlinear vibration analysis. The paper is structured as follows: in Section 2, we first review the intrinsic form of the geometrically nonlinear beam equations, which will be written in the compact form of Ref. [11]. Next, we will compute the linear normal modes of the system about an arbitrary fixed point of the system (that is, the static equilibrium under non-zero forces). Section 4 will introduce the nonlinear dynamics in modal coordinates around that fixed point. Different energy measures that are conserved in either time or space in the free vibrations of the structure are then identified in Sections 5 and 6. In the case of free vibrations about a non-zero equilibrium position, it is first shown that the total energy is generally not conserved. However, in this situation, sufficient conditions are presented to ensure the existence of a conserved quantity for constant follower forces by means of Casimir functions. Finally, Section 7 includes several numerical examples to illustrate the main findings of this work. They correspond to cantilever beams in large-amplitude free vibrations and under periodic loads.

2. Intrinsic beam equations

Following Cosserat's model, a beam of length S is defined by the rigid motion of cross-sections linked to a deformable reference line. This line needs not be straight, and its curvilinear coordinate in the reference configuration is the arc-length parameter s. The components of the local initial curvature vector in a local reference frame will be denoted as $\mathbf{k}_0(s)\in\mathbb{R}^3$. There will be no assumptions in terms of material or geometric characteristics of the cross section other than its area being small compared to the square of the typical scale in the beam deformations. The material constants are the cross-sectional mass matrix $\mathbf{M}$, and the flexibility (or compliance) matrix $\mathbf{C}$, both of which are obtained from a structural homogenization process [22]. They are full 6×6 symmetric matrices (including, in general, rotational inertia and transverse shear stiffness) that may vary with the arc length s, although we do not make this dependence explicit. The intrinsic equations that describe the beam dynamics under given applied forces, $\mathbf{f}_a(s,t)\in\mathbb{R}^3$, and moments, $\mathbf{m}_a(s,t)\in\mathbb{R}^3$, per unit length were developed by Hodges [13]. Defining the vector of applied loads as $\mathbf{f}_1(s,t)=\mathbf{f}_a;\mathbf{m}_a$, they will be written here in the compact form of Ref. [11] as

$$\begin{aligned}\mathbf{M}\dot{\mathbf{x}}_1-\mathbf{x}_2'-\mathbf{E}\mathbf{x}_2+\mathcal{L}_1(\mathbf{x}_1)\mathbf{M}\mathbf{x}_1+\mathcal{L}_2(\mathbf{x}_2)C\mathbf{x}_2=\mathbf{f}_1,\\ \mathbf{C}\dot{\mathbf{x}}_2-\mathbf{x}_1'+\mathbf{E}^{\top}\mathbf{x}_1-\mathcal{L}_1^{\top}(\mathbf{x}_1)\mathbf{C}\mathbf{x}_2=0.\end{aligned}\tag{1}$$

Dots ($\dot{\bullet}$) denote derivatives with respect to time, t, while primes ($\bullet'$) denote derivatives with respect to the arc length s. The state vector components $\mathbf{x}_1(s,t)\in\mathbb{R}^6$ and $\mathbf{x}_2(s,t)\in\mathbb{R}^6$ are defined as

$$\mathbf{x}_1=\begin{pmatrix}\mathbf{v}\\ \boldsymbol{\omega}\end{pmatrix},\quad \mathbf{x}_2=\begin{pmatrix}\mathbf{f}\\ \mathbf{m}\end{pmatrix},\tag{2}$$

where $\mathbf{v}(s,t)$ and $\boldsymbol{\omega}(s,t)$ are the local translational and angular inertial velocities; $\mathbf{f}(s,t)$ and $\mathbf{m}(s,t)$ are the sectional internal forces and moments, which are also often referred to as stress resultants. All vectors (including the applied forces, $\mathbf{f}_a$, and moments, $\mathbf{m}_a$) are defined in the current configuration and expressed in their components in the local (deformed) material frame. Therefore, constant values with time would denote constant following forces. The definition of the local velocities and stress resultants in terms of beam displacements and rotations can be found, for example, in Ref. [23], but will not be needed here.

The matrix $\mathbf{E}$ in Eq. (1) includes the effect of the initial twist and curvature and is defined as

$$\mathbf{E}:=\begin{pmatrix}\tilde{\mathbf{k}}_0 & 0\\ \tilde{\mathbf{e}}_1 & \tilde{\mathbf{k}}_0\end{pmatrix},\tag{3}$$

where $\mathbf{e}_1:=(1,0,0)$ and $\tilde{\bullet}$ is the skew-symmetric (or cross-product) operator, and the linear operators $\mathcal{L}_1$ and $\mathcal{L}_2$ are defined as

$$\mathcal{L}_1(\mathbf{x}_1):=\begin{pmatrix}\tilde{\boldsymbol{\omega}} & 0\\ \tilde{\mathbf{v}} & \tilde{\boldsymbol{\omega}}\end{pmatrix}\quad\text{and}\quad \mathcal{L}_2(x_2):=\begin{pmatrix}0 & \tilde{\mathbf{f}}\\ \tilde{\mathbf{f}} & \tilde{\mathbf{m}}\end{pmatrix}.\tag{4}$$

It can be easily seen that for each $\mathbf{h}_1,\mathbf{h}_2\in\mathbb{R}^6$, they satisfy

$$\mathcal{L}_1(\mathbf{h}_1)\mathbf{h}_2=\mathcal{L}_2(\mathbf{h}_2)\mathbf{h}_1,\tag{5}$$

$$\mathcal{L}_1^{\top}(\mathbf{h}_1)\mathbf{h}_2=-\mathcal{L}_1^{\top}(\mathbf{h}_2)\mathbf{h}_1.\tag{6}$$

Finally, it is worth comparing this description to others in the literature. The first equation in (1) corresponds to the linear- and angular-momentum balance equations, written in its intrinsic form. For static problems, it reduces to the equations of Reissner [24]. A full derivation of the dynamic equations can be found in the work by Simó [25]. The second equation in (1) is the compatibility condition between beam strains and velocities. It enforces that they correspond to the same displacement field, and thus ensures the uniqueness of the solution. Details of the derivation of this equation can be found in the work by Hodges [13]. The problem of numerically integrating Eq. (1) or otherwise characterizing its solutions must be solved with end conditions at $s=0$ and $s=S$, for all t, as well as with initial conditions for $\mathbf{x}_1$ and $\mathbf{x}_2$, for all s. The natural spatial boundary conditions satisfy[1]

$$\begin{aligned}x_{1,i}(0,t)x_{2,i}(0,t)=0,\\ x_{1,i}(S,t)x_{2,i}(S,t)=0,\end{aligned}\tag{7}$$

for $i=1,\ldots,6$. As it was mentioned in the Introduction, the intrinsic beam equations are related to Euler's rigid-body equations of motion. Indeed, a physical interpretation could be to consider the beam as a collection of rigid cross-sections moving as rigid bodies that are constrained by the internal forces and moments. Beam displacements and rotations would appear explicitly in the equations only if the applied forces and moments in Eq. (2), or the boundary conditions, depend on

[1] For a cantilever beam, the spatial boundary conditions are $\mathbf{x}_1(0,t)=0$ and $\mathbf{x}_2(S,t)=0$.

them. They can be obtained, at individual positions along the beam, by direct integration of the local velocities using methods of rigid-body dynamics [11].

3. Linear normal modes

In this section, we will obtain the linear normal modes (LNMs) of the system defined by (1) with boundary conditions such as those given in Eq. (7). Such LNMs will be used in subsequent sections to obtain a finite-dimensional description of the nonlinear beam dynamics. The LNMs of the undeformed beam have been derived in Ref. [11]. Here, we consider the more general case of the dynamics about a static equilibrium condition with a constant forcing $\overline{\mathbf{f}}_1$. The equilibrium state for the system (1) subject to such a forcing term is given by $\overline{\mathbf{x}}_1 = 0$, i.e., zero velocities, and a distribution of stress resultants $\overline{\mathbf{x}}_2(s)$ given by the solution to

$$\overline{\mathbf{x}}_2' + \mathbf{E}\overline{\mathbf{x}}_2 - \mathcal{L}_2(\overline{\mathbf{x}}_2)\mathbf{C}\overline{\mathbf{x}}_2 + \overline{\mathbf{f}}_1 = 0. \tag{8}$$

Once the static equilibrium is found, we can define the following perturbation states:

$$\delta\mathbf{x}_1 := \mathbf{x}_1,$$

$$\delta\mathbf{x}_2 := \mathbf{x}_2 - \overline{\mathbf{x}}_2. \tag{9}$$

Substituting this definition into Eq. (1) with zero additional loading gives the free vibrations around a static equilibrium (8). If we further assume small perturbations, it can be shown that the linearized beam dynamics around the equilibrium $\left(\begin{smallmatrix}0\\ \overline{\mathbf{x}}_2\end{smallmatrix}\right)$ are given by

$$\mathbf{M}\delta\dot{\mathbf{x}}_1 = \delta\mathbf{x}'_2 + [\mathbf{E} + \mathcal{L}_1(\mathbf{C}\overline{\mathbf{x}}_2) - \mathcal{L}_2(\overline{\mathbf{x}}_2)\mathbf{C}]\delta\mathbf{x}_2,$$

$$\mathbf{C}\delta\dot{\mathbf{x}}_2 = \delta\mathbf{x}'_1 - [\mathbf{E}^T + \mathcal{L}_1^T(\mathbf{C}\overline{\mathbf{x}}_2)]\delta\mathbf{x}_1, \tag{10}$$

where identities (5)–(6) were used to obtain the final expressions. Eq. (10) defines a homogeneous linear partial differential equation in the perturbation variables (9). Its solutions can be sought by inspection as in Ref. [18], that is,

$$\delta\mathbf{x}_1 = \boldsymbol{\phi}_{1j}(s)\sin(\omega_j t),$$

$$\delta\mathbf{x}_2 = \boldsymbol{\phi}_{2j}(s)\cos(\omega_j t). \tag{11}$$

As this is a first-order formulation, each LNM has associated mode shapes defined both in terms of velocities and resultant stresses. Consequently, substituting Eq. (11) into the homogeneous equation (10), defines an eigenvalue problem in the mode shape pairs $\boldsymbol{\phi}_j := \left(\begin{smallmatrix}\boldsymbol{\phi}_{1j}\\ \boldsymbol{\phi}_{2j}\end{smallmatrix}\right)$, as

$$(L + T)\boldsymbol{\phi}_j = \omega_j\boldsymbol{\phi}_j, \tag{12}$$

where we have defined the differential operator

$$L(\mathbf{g}) := \begin{pmatrix} 0 & \mathbf{M}^{-1} \\ -\mathbf{C}^{-1} & 0 \end{pmatrix}\begin{pmatrix} \mathbf{g}'_1 \\ \mathbf{g}'_2 \end{pmatrix}, \quad \mathbf{g} := \begin{pmatrix} \mathbf{g}_1 \\ \mathbf{g}_2 \end{pmatrix} \in D(S), \tag{13}$$

on an appropriate domain,[2] $D(S)$, and the bounded matrix operator

$$T := \begin{pmatrix} 0 & \mathbf{M}^{-1}(\mathbf{E} - \mathcal{L}_2(\overline{\mathbf{x}}_2)\mathbf{C} + \mathcal{L}_1(\mathbf{C}\overline{\mathbf{x}}_2)) \\ \mathbf{C}^{-1}(\mathbf{E}^T + \mathcal{L}_1^T(\mathbf{C}\overline{\mathbf{x}}_2)) & 0 \end{pmatrix}. \tag{14}$$

In Section 4, solutions to the nonlinear beam dynamic equations are constructed in terms of the mode shapes $\boldsymbol{\phi}_j$ using a Galerkin projection method. It is therefore of interest to determine whether the mode shapes $\boldsymbol{\phi}_j$ are orthogonal, which is equivalent to asking whether $L + T$ is a self-adjoint operator. Note first that, if elements of $D(S)$ satisfy the boundary conditions (7), L is self-adjoint with respect to the inner product

$$\langle \mathbf{h}, \mathbf{g} \rangle_{\mathbf{M},\mathbf{C}} := \int_0^S (\mathbf{h}_1^{\mathrm{T}}\mathbf{M}\mathbf{g}_1 + \mathbf{h}_2^{\mathrm{T}}\mathbf{C}\mathbf{g}_2)\,\mathrm{d}s. \tag{15}$$

On the other hand, the bounded operator T is self-adjoint with respect to $\langle \cdot, \cdot \rangle_{\mathbf{M},\mathbf{C}}$ if and only if

$$\int_0^S \mathbf{h}_2^{\mathrm{T}}\mathcal{L}_2^{\mathrm{T}}(\overline{\mathbf{x}}_2)\mathbf{C}\mathbf{g}_1\,\mathrm{d}s = \int_0^S \mathbf{h}_1^{\mathrm{T}}\mathcal{L}_2(\overline{\mathbf{x}}_2)\mathbf{C}\mathbf{g}_2\,\mathrm{d}s, \quad \forall \begin{pmatrix} \mathbf{g}_1 \\ \mathbf{g}_2 \end{pmatrix}, \begin{pmatrix} \mathbf{h}_1 \\ \mathbf{h}_2 \end{pmatrix}. \tag{16}$$

This condition holds if and only if $\overline{\mathbf{x}}_2 = 0$.

Using these results, we can now comment in detail how the properties of the operators L and T influence whether the spatial mode shapes $\boldsymbol{\phi}_j$ define an orthogonal set.

[2] For a cantilever beam, $D(S) := \{\mathbf{g} : \mathbf{g}_1', \mathbf{g}_2' \in L^2([0,S])^6, \mathbf{g}_1(0) = 0, \mathbf{g}_2(S) = 0\} \subset L^2([0,S])^6 \times L^2([0,S])^6$.

3.1. Undeformed initial equilibrium

In the case of an undeformed initial equilibrium $\overline{\mathbf{x}}_2 = 0$, $L+T$ is self-adjoint and hence has an orthonormal basis of eigenvectors satisfying

$$\langle \boldsymbol{\phi}_{1i}, \mathbf{M}\boldsymbol{\phi}_{1j}\rangle = \delta_{ij} = \langle \boldsymbol{\phi}_{2i}, \mathbf{C}\boldsymbol{\phi}_{2j}\rangle, \quad i,j\in\mathbb{N}, \tag{17}$$

where $\langle \mathbf{f}, \mathbf{g}\rangle := \int_0^S \mathbf{f}^{\mathrm{T}}\mathbf{g}\,\mathrm{d}s$ is the standard L^2-inner product on $L^2([0,S])^6$.

3.2. Deformed initial equilibrium

In the case of a deformed initial equilibrium, i.e., $\overline{\mathbf{x}}_2 \neq 0$, the operator T is no longer self-adjoint. However, since $L+T$ is a bounded perturbation of a self-adjoint operator, relatively mild conditions exist [26] under which $L+T$ has a complete set of eigenvectors $\boldsymbol{\phi}_j$, for which both $(\boldsymbol{\phi}_{1j})_{j=1}^{\infty}$ and $(\boldsymbol{\phi}_{2j})_{j=1}^{\infty}$ span $L^2([0,S])^6$. If this is the case then the orthogonality condition (17) cannot hold, in contrast to the undeformed equilibrium. To see why this is true, note that if (17) holds then Eq. (12) can be used to show that

$$\langle \boldsymbol{\phi}_{1i}, \mathcal{L}_2(\overline{\mathbf{x}}_2)\mathbf{C}\boldsymbol{\phi}_{2j}\rangle = 0, \quad \forall (i,j)\in\mathbb{N}\times\mathbb{N}. \tag{18}$$

Since the eigenvectors span $L^2([0,S])^6$ it follows that $\mathcal{L}_2(\overline{\mathbf{x}}_2)\mathbf{C} = 0$ and hence, $\overline{\mathbf{x}}_2 = 0$.

In summary, assuming that $L+T$ has a complete set of eigenvectors, the orthonormality conditions (17) are true if and only if the reference conditions correspond to the undeformed beam.

4. Nonlinear equations of motion in intrinsic modal coordinates

The mode shapes $\boldsymbol{\phi}_j$ obtained in the previous section will now be used to construct solutions of the partial differential equation (1) by writing the states of the intrinsic model in the separated form

$$\mathbf{x}_1(t,s) = \sum q_{1j}(t)\boldsymbol{\phi}_{1j}(s),$$

$$\mathbf{x}_2(t,s) = \sum q_{2j}(t)\boldsymbol{\phi}_{2j}(s) + \overline{\mathbf{x}}_2(s). \tag{19}$$

Substituting this Ansatz into Eq. (1) and projecting the results onto each of the modal functions, $\boldsymbol{\phi}_j$, results in the following system of ODEs for the temporal weighting functions $\mathbf{q}_1(t) := (q_{11}; q_{12}; \ldots)$ and $\mathbf{q}_2(t) := (q_{21}; q_{22}; \ldots)$:

$$\mathbf{A}_1\dot{\mathbf{q}}_1 = \mathbf{B}_1\mathbf{q}_2 - (q_{1\ell}\boldsymbol{\Gamma}_1^{\ell}\mathbf{q}_1 + q_{2\ell}\boldsymbol{\Gamma}_2^{\ell}\mathbf{q}_2) + \boldsymbol{\eta}_1$$

$$\mathbf{A}_2\dot{\mathbf{q}}_2 = \mathbf{B}_2\mathbf{q}_1 + q_{2\ell}(\boldsymbol{\Gamma}_2^{\ell})^{\mathrm{T}}\mathbf{q}_1, \tag{20}$$

where we have used Einstein's summation convention on repeated indices. The coefficients in this equation are the real constants

$$(\mathbf{A}_1)_{jk} := \langle \boldsymbol{\phi}_{1j}, \mathbf{M}\boldsymbol{\phi}_{1k}\rangle$$

$$(\mathbf{A}_2)_{jk} := \langle \boldsymbol{\phi}_{2j}, \mathbf{C}\boldsymbol{\phi}_{2k}\rangle$$

$$(\mathbf{B}_1)_{jk} := \langle \boldsymbol{\phi}_{1j}, \boldsymbol{\phi}'_{2k} + (\mathbf{E} - \mathcal{L}_2(\overline{\mathbf{x}}_2)\mathbf{C} + \mathcal{L}_1(\mathbf{C}\overline{\mathbf{x}}_2))\boldsymbol{\phi}_{2k}\rangle$$

$$(\mathbf{B}_2)_{jk} := \langle \boldsymbol{\phi}_{2j}, \boldsymbol{\phi}'_{1k} - (\mathbf{E}^T + \mathcal{L}_1^T(\mathbf{C}\overline{\mathbf{x}}_2))\boldsymbol{\phi}_{1k}\rangle$$

$$(\boldsymbol{\Gamma}_1^{\ell})_{jk} := \langle \boldsymbol{\phi}_{1j}, \mathcal{L}_1(\boldsymbol{\phi}_{1k})\mathbf{M}\boldsymbol{\phi}_{1\ell}\rangle$$

$$(\boldsymbol{\Gamma}_2^{\ell})_{jk} := \langle \boldsymbol{\phi}_{1j}, \mathcal{L}_2(\boldsymbol{\phi}_{2k})\mathbf{C}\boldsymbol{\phi}_{2\ell}\rangle$$

$$\eta_{1j} := \langle \boldsymbol{\phi}_{1j}, \mathbf{f}_1 - \overline{\mathbf{f}}_1\rangle. \tag{21}$$

Note that all these coefficients are constant functions of the problem data and consequently can be pre-computed offline, and that they completely characterize the geometrically exact beam dynamic equations in modal coordinates. Using Eq. (6), it can be shown that each of the matrices $\boldsymbol{\Gamma}_1^{\ell}$ is antisymmetric. Moreover, since $\mathbf{M}$ and $\mathbf{C}$ are symmetric matrices, it follows that $\mathbf{A}_1$ and $\mathbf{A}_2$ are symmetric. Note finally that these equations simplify to those of Ref. [11, Eq. (20)] when $\overline{\mathbf{x}}_2 = 0$, since in this case (17) implies that $\mathbf{A}_1 = \mathbf{I}$ and $\mathbf{A}_2 = \mathbf{I}$.

Since, in general, the mode shapes do not define an orthogonal set, Eq. (20) is still valid for any other suitable basis $\boldsymbol{\phi}_j(s)$. This includes, in particular, a finite-element discretization of the curvilinear domain, as it was done in Ref. [23].

5. Quantities conserved with time

We can now identify various energy metrics in the equations that describe the geometrically nonlinear beam dynamics. The most obvious one is the *total energy* of the system (1), which is defined in the usual way as the sum of the instantaneous kinetic and strain energy,

$$\mathcal{E}_0(\mathbf{x}_1,\mathbf{x}_2) := \tfrac{1}{2}\langle \mathbf{x}_1, \mathbf{M}\mathbf{x}_1\rangle + \tfrac{1}{2}\langle \mathbf{x}_2, \mathbf{C}\,\mathbf{x}_2\rangle. \tag{22}$$

It is easily shown from Eq. (1) that the energy dissipation rate is given by the instantaneous mechanical power of the external forces, i.e.,

$$\frac{\mathrm{d}\mathcal{E}_0}{\mathrm{d}t} = \langle \mathbf{x}_1, \mathbf{f}_1\rangle, \tag{23}$$

which implies, as expected, that the free vibrations of the unforced system are energy-invariant. Next, consider the perturbations of a system initially in static equilibrium with constant forcing $\bar{\mathbf{f}}_1$, defined by Eq. (8). Its subsequent dynamics —keeping all nonlinear terms—is written in terms of the perturbation states (9) as

$$\begin{aligned} \mathbf{M}\delta\dot{\mathbf{x}}_1 - \delta\mathbf{x}_2{}' - \mathbf{E}\delta\mathbf{x}_2 + \mathcal{L}_2(\delta\mathbf{x}_2)\mathbf{C}\bar{\mathbf{x}}_2 + \mathcal{L}_2(\bar{\mathbf{x}}_2)\mathbf{C}\delta\mathbf{x}_2 + \mathcal{L}_1(\delta\mathbf{x}_1)\mathbf{M}\delta\mathbf{x}_1 + \mathcal{L}_2(\delta\mathbf{x}_2)\mathbf{C}\delta\mathbf{x}_2 = 0,\\ \mathbf{C}\delta\dot{\mathbf{x}}_2 - \delta\mathbf{x}_1{}' + \mathbf{E}^{\top}\delta\mathbf{x}_1 - \mathcal{L}_1^{\top}(\delta\mathbf{x}_1)\mathbf{C}\bar{\mathbf{x}}_2 - \mathcal{L}_1^{\top}(\delta\mathbf{x}_1)\mathbf{C}\delta\mathbf{x}_2 = 0. \end{aligned} \tag{24}$$

From Eq. (23), the total energy of this forced system is not conserved. We can define instead its *perturbation energy* about the equilibrium condition $\bar{\mathbf{x}}_2$, by analogy with the total energy, as

$$\mathcal{E}_{\bar{\mathbf{x}}_2}(\delta\mathbf{x}_1,\delta\mathbf{x}_2) := \tfrac{1}{2}\langle \delta\mathbf{x}_1, \mathbf{M}\delta\mathbf{x}_1\rangle + \tfrac{1}{2}\langle \delta\mathbf{x}_2, \mathbf{C}\delta\mathbf{x}_2\rangle. \tag{25}$$

Since the underlying partial differential equation (24) is nonlinear, it should not be expected that (25) is invariant, except in the unforced case $\bar{\mathbf{x}}_2 = 0$. Indeed,

$$\begin{aligned} \frac{\mathrm{d}\mathcal{E}_0}{\mathrm{d}t} - \frac{\mathrm{d}\mathcal{E}_{\bar{\mathbf{x}}_2}}{\mathrm{d}t} &= \langle \mathbf{C}\delta\dot{\mathbf{x}}_2, \bar{\mathbf{x}}_2\rangle = \langle \delta\mathbf{x}'_1 - \mathbf{E}^{\top}\delta\mathbf{x}_1 + \mathcal{L}_1^{\top}(\delta\mathbf{x}_1)\mathbf{C}\bar{\mathbf{x}}_2 + \mathcal{L}_1^{\top}(\delta\mathbf{x}_1)\mathbf{C}\delta\mathbf{x}_2, \bar{\mathbf{x}}_2\rangle\\ &= \langle \delta\mathbf{x}_1, -\bar{\mathbf{x}}'_2 - \mathbf{E}\bar{\mathbf{x}}_2 + \mathcal{L}_2(\bar{\mathbf{x}}_2)\mathbf{C}\bar{\mathbf{x}}_2\rangle - \langle \mathcal{L}_1(\delta\mathbf{x}_1)\mathbf{C}\delta\mathbf{x}_2, \bar{\mathbf{x}}_2\rangle\\ &(\text{by } (8)) = \langle \delta\mathbf{x}_1, \bar{\mathbf{f}}_1\rangle - \langle \mathcal{L}_1(\delta\mathbf{x}_1)\mathbf{C}\delta\mathbf{x}_2, \bar{\mathbf{x}}_2\rangle. \end{aligned} \tag{26}$$

Hence, and noting that $\delta\mathbf{x}_1 = \mathbf{x}_1$ for perturbations about static equilibrium, the expression (23) for the energy dissipation of the original system can be used to show that

$$\frac{\mathrm{d}\mathcal{E}_{\bar{\mathbf{x}}_2}}{\mathrm{d}t} = \langle \mathcal{L}_1(\delta\mathbf{x}_1)\mathbf{C}\delta\mathbf{x}_2, \bar{\mathbf{x}}_2\rangle, \tag{27}$$

meaning that the energy dissipation rate corresponding to the perturbation states depends upon the interaction of the gyroscopic term $\mathcal{L}_1(\delta\mathbf{x}_1)\mathbf{C}\delta\mathbf{x}_2$ (a cross product of the local angular velocity and the local beam strains) with the stress resultants at the equilibrium position, $\bar{\mathbf{x}}_2$. In general, the above expression is non-zero and hence the perturbation energy $\mathcal{E}_{\bar{\mathbf{x}}_2}$ is not time-invariant in the free vibrations about a non-zero equilibrium condition. This result may still be useful, as Eq. (27) gives the rate of change of the perturbation energy in the same way in which Eq. (23) gave the rate of change of the total energy.

5.1. Energy in the free vibrations of the approximating finite-dimensional systems

It is now of interest to determine whether the energy conservation and dissipation properties of the full PDE, initially in static equilibrium under constant forcing, Eq. (24), are inherited by its finite-dimensional approximations. As before, assume that Eq. (24) has solutions of the form

$$\delta\mathbf{x}_1 = \sum_{j=1}^{N} q_{1j}(t)\boldsymbol{\phi}_{1j}(s), \quad \delta\mathbf{x}_2 = \sum_{j=1}^{N} q_{2j}(t)\boldsymbol{\phi}_{2j}(s), \tag{28}$$

for spatial mode shapes $\boldsymbol{\phi}_j(s)$ satisfying the eigenvalue problem (12) and temporal weighting functions $\binom{q_{1j}}{q_{2j}}$ satisfying the ordinary differential equations (20). That is, solutions of the continuous problem are found using a projection on a finite-number of mode shapes. The states in this ODE (20) will be written as

$$\mathbf{q}_1 := (q_{11};\ldots;q_{1N}), \quad \mathbf{q}_2 := (q_{21};\ldots;q_{2N}). \tag{29}$$

An energy-type quantity can be defined for each of the finite-dimensional systems as

$$\mathcal{E}^N_{\bar{\mathbf{x}}_2}(\mathbf{q}_1,\mathbf{q}_2) := \tfrac{1}{2}(\mathbf{q}_1^{\top}\mathbf{A}_1\mathbf{q}_1 + \mathbf{q}_2^{\top}\mathbf{A}_2\mathbf{q}_2). \tag{30}$$

This is the natural finite-dimensional analogue of the perturbation energy, $\mathcal{E}_{\bar{\mathbf{x}}_2}(\delta\mathbf{x}_1,\delta\mathbf{x}_2)$, since, by definition of $\mathbf{A}_1$ and $\mathbf{A}_2$ in (21), Eq. (30) is directly obtained by substituting the modal expansions (28) into Eq. (25). Note that the matrices $\mathbf{A}_1, \mathbf{A}_2$ depend implicitly on the forcing $\bar{\mathbf{f}}_1$ since the mode shapes $\boldsymbol{\phi}_j$ are defined (by Eq. (12)) in terms of the equilibrium point $\binom{0}{\bar{\mathbf{x}}_2}$.

An important special case is when $\overline{\mathbf{f}}_1 = 0$, which implies $\overline{\mathbf{x}}_2 = 0$ and that the modes $\boldsymbol{\phi}_j(s)$ satisfy (17). As discussed in section 4, in this special case we have $\mathbf{A}_1 = I = \mathbf{A}_2$ and, consequently, the energy of each finite-dimensional ODE approximating Eq. (1) is

$$\mathcal{E}_0^N(\mathbf{q}_1, \mathbf{q}_2) = \frac{1}{2}\sum_{j=1}^{N}(\mathbf{q}_{1j}^2 + \mathbf{q}_{2j}^2). \tag{31}$$

In the following section, it will be shown that the energy invariance of the unforced system, that was determined in Eq. (23), is inherited by each of its finite-dimensional approximations, i.e., that $\mathrm{d}\mathcal{E}_0^N/\mathrm{d}t = 0$, for each approximation dimension N. Similarly, for the case of an initially deformed configuration, the energy $\mathcal{E}_{\overline{\mathbf{x}}_2}^N$ will be shown to have a dissipation rate analogous to Eq. (27). To this end, using (20), the derivative of the ODE energy (30) is given by

$$\begin{aligned}\frac{\mathrm{d}\mathcal{E}_{\overline{\mathbf{x}}_2}^N}{\mathrm{d}t} &= \mathbf{q}_1^\top \mathbf{A}_1 \dot{\mathbf{q}}_1 + \mathbf{q}_2^\top \mathbf{A}_2 \dot{\mathbf{q}}_2 = \mathbf{q}_1^\top(\mathbf{B}_1 + \mathbf{B}_2^\top)\mathbf{q}_2 \\ -q_{1\ell}\mathbf{q}_1^\top \boldsymbol{\Gamma}_1^{\ell}\mathbf{q}_1 - q_{2\ell}(\mathbf{q}_1^\top \boldsymbol{\Gamma}_2^{\ell}\mathbf{q}_2 - \mathbf{q}_2^\top(\boldsymbol{\Gamma}_2^{\ell})^\top \mathbf{q}_1) &= \mathbf{q}_1^\top(\mathbf{B}_1 + \mathbf{B}_2^\top)\mathbf{q}_2,\end{aligned} \tag{32}$$

where the final equality holds since each $\boldsymbol{\Gamma}_1^{\ell}$ is anti-symmetric. One can use this expression to study the energy-invariance characteristics of the free vibration about each of the two cases for the initial equilibrium.

5.1.1. Energy invariance for an unloaded initial equilibrium, $\overline{\mathbf{x}}_2 = 0$

In the undeformed case, the orthogonality relations (17) imply that $\mathbf{A}_1 = I = \mathbf{A}_2$. Furthermore, since the mode shapes $\boldsymbol{\phi}_j(s)$ satisfy (12) with $\overline{\mathbf{x}}_2 = 0$, it can be seen that $\mathbf{B}_1 = \boldsymbol{\Omega} = -\mathbf{B}_2$, where $\boldsymbol{\Omega} := \mathrm{diag}(\omega_1, \ldots, \omega_N)$. It follows from (32) that

$$\frac{\mathrm{d}\mathcal{E}_0^N}{\mathrm{d}t} = \mathbf{q}_1^\top(\boldsymbol{\Omega} - \boldsymbol{\Omega})\mathbf{q}_2 = 0. \tag{33}$$

Hence, each finite-dimensional approximation of the undeformed system is energy-invariant. Note that energy invariance of the finite-dimensional system holds regardless of the quality (accuracy) of the approximation that it provides to the actual dynamics of the full system. This energy conservation will be shown numerically in Section 7 for the nonlinear free vibrations of a cantilever beam.

5.1.2. Energy-dissipation rate for a deformed equilibrium, $\overline{\mathbf{x}}_2 \neq 0$

The energy of the perturbation states in the deformed case $\overline{\mathbf{x}}_2 \neq 0$ satisfies

$$\frac{\mathrm{d}\mathcal{E}_{\overline{\mathbf{x}}_2}^N}{\mathrm{d}t} = \mathbf{q}_1^\top(\mathbf{B}_1 + \mathbf{B}_2^\top)\mathbf{q}_2. \tag{34}$$

Using (21), it can be shown that

$$(\mathbf{B}_1 + \mathbf{B}_2^\top)_{jk} = \langle \mathcal{L}_2(\boldsymbol{\phi}_{1j})\mathbf{C}\boldsymbol{\phi}_{2j}, \overline{\mathbf{x}}_2 \rangle \tag{35}$$

which provides the finite-dimensional analogue to Eq. (27). It can also be deduced from (21) that $\mathbf{B}_1 = \mathbf{A}_1\boldsymbol{\Omega}$ and $\mathbf{B}_2 = -\mathbf{A}_2\boldsymbol{\Omega}$ and hence,

$$\frac{\mathrm{d}\mathcal{E}_{\overline{\mathbf{x}}_2}^N}{\mathrm{d}t} = \mathbf{q}_1^\top(\mathbf{A}_1\boldsymbol{\Omega} - \boldsymbol{\Omega}\mathbf{A}_2)\mathbf{q}_2. \tag{36}$$

In general, $\mathbf{A}_1\boldsymbol{\Omega} \neq \boldsymbol{\Omega}\mathbf{A}_2$ and the energy $\mathcal{E}_{\overline{\mathbf{x}}_2}^N$ is not invariant. Note however that, *if* the energy $\mathcal{E}_{\overline{\mathbf{x}}_2}^N$ were invariant (i.e., if $\mathbf{A}_1\boldsymbol{\Omega} = \boldsymbol{\Omega}\mathbf{A}_2$), then trajectories of the (20) would lie on the surface of the ellipse

$$\left\{ \begin{pmatrix} \mathbf{q}_1 \\ \mathbf{q}_2 \end{pmatrix} : \|\mathbf{A}_1^{1/2}\mathbf{q}_1\|^2 + \|\mathbf{A}_2^{1/2}\mathbf{q}_2\|^2 = 2K \right\} \subset \mathbb{R}^{2N}, \tag{37}$$

with K the perturbation energy at $t = 0$. In the next section we develop a more general method, based on constructing Casimir functions, for searching for invariant quantities of the forced system dynamics.

5.2. Conserved quantities under constant forcing via Casimir functions

In the case of a deformed equilibrium, $\overline{\mathbf{x}}_2 \neq 0$, it was shown in the previous section that the perturbation energy $\mathcal{E}_{\overline{\mathbf{x}}_2}^N$ associated with the finite-dimensional approximation to the forced PDE (1) is not invariant in general.[3] A different approach towards approximating the forced PDE is therefore needed. In particular, we employ Casimir functions [27] to derive conditions for the existence of conserved quantities in this case.

To achieve this, we will need first to project the system of equations (1) on the mode shapes $\boldsymbol{\phi}_j$ satisfying (12) for $\overline{\mathbf{x}}_2 = 0$, that is, we make the substitution $\mathbf{x}_1 = \sum q_{1i}\boldsymbol{\phi}_{1i}, \mathbf{x}_2 = \sum q_{2i}\boldsymbol{\phi}_{2i}$ and project by taking the inner product with each mode shape.

[3] Note that due to the constant forcing $\overline{\mathbf{f}}_1$ in (23), the total energy $\mathcal{E}_0^N$ is not invariant either.

This results in a forced ODE approximation of the form

$$\dot{\mathbf{q}}_1 = \boldsymbol{\Omega}\mathbf{q}_2 - (q_{1\ell}\boldsymbol{\Gamma}_1^{\ell}\mathbf{q}_1 + q_{2\ell}\boldsymbol{\Gamma}_2^{\ell}\mathbf{q}_2) + \overline{\boldsymbol{\eta}}_1,$$

$$\dot{\mathbf{q}}_2 = -\boldsymbol{\Omega}\mathbf{q}_1 + q_{2\ell}(\boldsymbol{\Gamma}_2^{\ell})^{\top}\mathbf{q}_1, \tag{38}$$

where $\overline{\eta}_{1j} := \langle \boldsymbol{\phi}_{1j}, \overline{\mathbf{f}}_1 \rangle$ are constant coefficients and the matrices appearing in (38) are defined as in Eq. (21) with $\overline{\mathbf{x}}_2 = 0$. In other words, the original, forced, partial differential equation (1) is approximated using a forced ODE. This is in contrast to the approach taken in Section 4, where the PDE itself was first linearized about the deformed equilibrium condition.

The drawback of this approach is, of course, that the linearization of Eq. (38) no longer represents the small amplitude oscillations about the (nonlinear) static equilibrium. However, the resulting dynamical system is a *forced Hamiltonian system*, for which analysis methods are readily available in the literature [14]. Writing $\mathbf{q} = \binom{\mathbf{q}_1}{\mathbf{q}_2}$, Eq. (38) can be written as

$$\dot{\mathbf{q}} = (\mathbf{W} + \mathbf{N}(\mathbf{q}))\mathbf{q} + \begin{pmatrix} \overline{\boldsymbol{\eta}}_1 \\ 0 \end{pmatrix}, \tag{39}$$

where

$$\mathbf{W} := \begin{pmatrix} 0 & \boldsymbol{\Omega} \\ -\boldsymbol{\Omega} & 0 \end{pmatrix}, \quad \mathbf{N}(\mathbf{q}) := \begin{pmatrix} -\mathbf{N}_1(\mathbf{q}_1) & -\mathbf{N}_2(\mathbf{q}_2) \\ \mathbf{N}_2(\mathbf{q}_2)^{\top} & 0 \end{pmatrix}, \tag{40}$$

where $\mathbf{N}_1(\mathbf{q}_1) := q_{1\ell}\boldsymbol{\Gamma}_1^{\ell}$ and $\mathbf{N}_2(\mathbf{q}_2) := q_{2\ell}\boldsymbol{\Gamma}_2^{\ell}$. Properties of the forced system (38) can now be deduced using the particular Hamiltonian structure of the system matrices (40). Since $\boldsymbol{\Omega}$ is diagonal and each $\boldsymbol{\Gamma}_1^{\ell}$ is anti-symmetric, it follows that $\mathbf{W} + \mathbf{N}(\mathbf{q})$ is antisymmetric for each $\mathbf{q} \in \mathbb{R}^{2N}$. It is also not difficult to verify that the equilibrium solutions $\overline{\mathbf{q}} \in \mathbb{R}^{2N}$ of this forced non-dissipative system are of the form $\overline{\mathbf{q}} = \binom{0}{\overline{\mathbf{q}}_2}$, with $\overline{\mathbf{q}}_2$ satisfying

$$\overline{\mathbf{q}}_2 = (-\boldsymbol{\Omega} + \mathbf{N}_2(\overline{\mathbf{q}}_2))^{-1}\overline{\boldsymbol{\eta}}_1. \tag{41}$$

We now provide a sufficient condition for the existence of an invariant quantity for trajectories of the forced system (38) about such an equilibrium position. Again motivated by Ref. [14], define the candidate Lyapunov function

$$V(\mathbf{q}) := \tfrac{1}{2}\|\mathbf{q}\|_2^2 - \overline{\boldsymbol{\eta}}_1^{\top}\mathcal{C}(\mathbf{q}_2), \quad \mathbf{q} = \begin{pmatrix} \mathbf{q}_1 \\ \mathbf{q}_2 \end{pmatrix}, \tag{42}$$

where $\mathcal{C} : \mathbb{R}^N \to \mathbb{R}^N$ is a function which depends only upon the second component of the state $\mathbf{q}_2$. The derivative of V along trajectories of (38) is given by[4]

$$\frac{\mathrm{d}V}{\mathrm{d}t} = \frac{\partial V}{\partial \mathbf{q}}\dot{\mathbf{q}} = \left(\mathbf{q}^{\top} - \left[0 : \overline{\boldsymbol{\eta}}_1^{\top}\frac{\partial \mathcal{C}}{\partial \mathbf{q}_2}\right]\right)\left((\mathbf{W} + \mathbf{N}(\mathbf{q}))\mathbf{q} + \begin{pmatrix} \overline{\boldsymbol{\eta}}_1 \\ 0 \end{pmatrix}\right),$$

$$(\text{by (40)} = \mathbf{q}_1^{\top}\overline{\boldsymbol{\eta}}_1 - \left[\overline{\boldsymbol{\eta}}_1^{\top}\frac{\partial \mathcal{C}}{\partial \mathbf{q}_2}(-\boldsymbol{\Omega} + \mathbf{N}_2(\mathbf{q}_2)^{\top}) : 0\right]\mathbf{q}$$

$$= \mathbf{q}_1^{\top}\overline{\boldsymbol{\eta}}_1 - \overline{\boldsymbol{\eta}}_1^{\top}\frac{\partial \mathcal{C}}{\partial \mathbf{q}_2}(-\boldsymbol{\Omega} + N_2(\mathbf{q}_2)^{\top})\mathbf{q}_1. \tag{43}$$

Consequently, if there exists a function $\mathcal{C} : \mathbb{R}^N \to \mathbb{R}^N$ that satisfies the partial differential equation

$$\frac{\partial \mathcal{C}}{\partial \mathbf{q}_2} = (-\boldsymbol{\Omega} + N_2(\mathbf{q}_2)^{\top})^{-1}, \quad \mathbf{q}_2 \in \mathbb{R}^N, \tag{44}$$

then $\mathrm{d}V/\mathrm{d}t = 0$ along trajectories of the forced system. Hence, the quantity $V(\mathbf{q}(t))$ is preserved in time.

A function $\mathcal{C}$ satisfying (44) is called a *Casimir function* [27]. If a Casimir function can be constructed then, depending on the inherited properties of V, information can be deduced about trajectories of the forced system. For example, if $\mathcal{C}$ is linear (which occurs if $\mathbf{N}_2 \equiv 0$) then

$$V(\mathbf{q}(t)) = \tfrac{1}{2}\|\mathbf{q}(t) - \overline{\mathbf{q}}\|_2^2 = \tfrac{1}{2}\|\mathbf{q}_1\|_2^2 + \tfrac{1}{2}\|\mathbf{q}_1 + \boldsymbol{\Omega}^{-1}\overline{\boldsymbol{\eta}}_1\|_2^2 \tag{45}$$

and each trajectory of the forced system lies on the surface of an sphere in $\mathbb{R}^{2N}$ centred at $\overline{\mathbf{q}}$. More generally, if V is positive definite then trajectories of (38) lie on closed contours of $\mathbb{R}^N$ (the level sets of V). Note also that if $\mathcal{C}$ is a Casimir then, since each equilibrium position $\overline{\mathbf{q}}$ of the system satisfies (41), it follows that

$$\frac{\partial V}{\partial \mathbf{q}}(\overline{\mathbf{q}}) = 0, \tag{46}$$

i.e., equilibrium points of the system are stationary points of V.

[4] For the sake of clarity, we employ the convention $[\partial \mathcal{C}/\partial \mathbf{q}_2]_{ij} := \partial \mathcal{C}_i/\partial q_{2j}$.

5.2.1. Existence of Casimir functions

In general, constructing a Casimir function $\mathcal{C}$ satisfying (44) is a difficult task and it is not always the case that such a function exists. To provide a condition for existence, note that $\mathbf{q}_2 \mapsto -\mathbf{\Omega} + \mathbf{N}(\mathbf{q}_2)^\top$ is a linear function of $\mathbf{q}_2$. Hence, there exists a matrix $R(\mathbf{q}_2) \in \mathbb{R}^{N\times N}$, each entry of which is a rational function[5] of $\mathbf{q}_2$, for which

$$(-\mathbf{\Omega} + \mathbf{N}(\mathbf{q}_2)^\top)^{-1} = \mathbf{R}(\mathbf{q}_2), \quad \mathbf{q}_2 \in \mathbb{R}^N. \tag{47}$$

Poincaré's Lemma implies that a Casimir function exists satisfying (44) if and only if

$$\frac{\partial R_{ij}}{\partial q_{2k}} = \frac{\partial R_{kj}}{\partial q_{2i}}, \quad i,j,k \in \{1,\ldots,N\}. \tag{48}$$

Now, for any matrix $\mathbf{A}$ which depends upon a scalar parameter z, $\partial \mathbf{A}^{-1}/\partial z = -\mathbf{A}^{-1}(\partial \mathbf{A}/\partial z)\mathbf{A}^{-1}$. Hence, (48) is equivalent to

$$(\mathbf{R}(\mathbf{q}_2)(\mathbf{\Gamma}_2^i)^\top \mathbf{R}(\mathbf{q}_2))_{kj} = (\mathbf{R}(\mathbf{q}_2)(\mathbf{\Gamma}_2^k)^\top R(\mathbf{q}_2))_{ij}, \quad i,j,k \in \{1,\ldots,N\}, \tag{49}$$

which holds if and only if

$$(\mathbf{R}(\mathbf{q}_2)(\mathbf{\Gamma}_2^i)^\top)_{kj} = (\mathbf{R}(\mathbf{q}_2)(\mathbf{\Gamma}_2^k)^\top)_{ij}, \quad i,j,k \in \{1,\ldots,N\}. \tag{50}$$

Since $\mathbf{R}(\mathbf{q}_2)$ can be calculated analytically, this condition can in principal be checked to verify the existence of a Casimir function for the forced dynamics (38). For alternative conditions characterizing the existence of solutions to Eq. (44), see Ref. [28].

We pose as an open question which, if any, conditions upon the structural matrices $\mathbf{M}, \mathbf{C}$ imply that (50) is satisfied.

5.2.2. Approximation of Casimir functions

In practice, computing an analytical expression for $\mathbf{R}(\mathbf{q}_2)$ may be difficult unless the state dimension N is small. If $\mathbf{R}(\mathbf{q}_2)$ cannot be calculated, we instead propose constructing an approximate Casimir function. Assuming $\|N_2(\mathbf{q}_2)\| < \|\mathbf{\Omega}\|$, which introduces an upper bound on the internal forces/moments, the inverse appearing in Eq. (44) may be written as

$$(-\mathbf{\Omega} + \mathbf{N}_2(\mathbf{q}_2)^\top)^{-1} = -\sum_{n=0}^{\infty} (\mathbf{\Omega}^{-1}\mathbf{N}_2(\mathbf{q}_2)^\top)^n \mathbf{\Omega}^{-1}. \tag{51}$$

Now, if $\mathcal{C}$ has the form $\mathcal{C} = \sum_{n=0}^{\infty} \mathcal{C}^{(n)}$ and

$$\frac{\partial \mathcal{C}^{(n)}}{\partial \mathbf{q}_2} = -(\mathbf{\Omega}^{-1}\mathbf{N}_2(\mathbf{q}_2)^\top)^n \mathbf{\Omega}^{-1}, \quad n \in \mathbb{N}\cup\{0\}. \tag{52}$$

it follows that $\mathcal{C}$ is a Casimir function.

As it will be seen in the numerical examples, it may be sufficient to compute only a finite number of terms $\mathcal{C}^{(n)}$ to observe preservation of the associated Lyapunov function V along trajectories of (20). We indicate how to calculate $\mathcal{C}^{(0)}$ and $\mathcal{C}^{(1)}$. For $n=0$, select

$$\mathcal{C}^{(0)}(\mathbf{q}_2) = -\mathbf{\Omega}^{-1}\mathbf{q}_2 \tag{53}$$

For $n=1$, suppose that $\mathcal{C}^{(1)}$ is a general quadratic polynomial in the variable $\mathbf{q}_2$, i.e.,

$$\mathcal{C}^{(1)}(\mathbf{q}_2) := \tfrac{1}{2}(\mathbf{q}_2^\top Q^{(i)}\mathbf{q}_2)_{i=1}^N, \quad \mathbf{Q}^{(i)} = (\mathbf{Q}^{(i)})^\top. \tag{54}$$

We want to select matrices $\mathbf{Q}^{(i)}$ such that

$$\frac{\partial \mathcal{C}^{(1)}}{\partial \mathbf{q}_2} = \begin{pmatrix} \mathbf{q}_2^\top \mathbf{Q}^{(1)} \\ \vdots \\ \mathbf{q}_2^\top \mathbf{Q}^{(\mathbf{N})} \end{pmatrix} = -\mathbf{\Omega}^{-1}\mathbf{N}_2(\mathbf{q}_2)^\top \mathbf{\Omega}^{-1} = \mathbf{q}_{2\ell}\mathbf{G}^{(\ell)} \tag{55}$$

where $G^{(\ell)} := -\mathbf{\Omega}^{-1}(\mathbf{\Gamma}_2^\ell)^\top \mathbf{\Omega}^{-1}$. Let

$$\mathbf{Q}^{(i)} := (q_{j\ell}^{(i)}) := \left(\frac{g_{ij}^{(\ell)} + g_{i\ell}^{(j)}}{2}\right). \tag{56}$$

A comparison of coefficients shows that (55) holds if

$$g_{ij}^{(\ell)} = g_{i\ell}^{(j)}, \quad i,j,\ell \in \{1,\ldots,N\} \tag{57}$$

Even if this is not the case, it can be shown that $\mathcal{C}^{(1)}$ is the unique quadratic function for which that ℓ^2-distance between the coefficients of $\partial \mathcal{C}^{(1)}/\partial \mathbf{q}_2$ and $-\mathbf{\Omega}^{-1}\mathbf{N}_2(\mathbf{q}_2)^\top \mathbf{\Omega}^{-1}$ is minimized.

[5] A function f is rational in q_2 if $f(\mathbf{q}_2) = a(\mathbf{q}_2)/b(\mathbf{q}_2)$ for polynomials $a, b : \mathbb{R}^{\mathbf{N}} \to \mathbb{R}$.

In Section 7, $V(\mathbf{q}) = \frac{1}{2}\|\mathbf{q}\|^2 - \boldsymbol{\eta}_1^\top \mathcal{C}(\mathbf{q}_2)$ is calculated for a numerical example of a cantilever beam vibrating freely about a non-zero equilibrium. The Casimir function $\mathcal{C}$ is approximated by $\mathcal{C} \approx \mathcal{C}^{(0)} + \mathcal{C}^{(1)}$ and the resulting trajectory of V is plotted in Fig. 6.

6. Spatial conservation laws

We consider finally spatial invariance of the *average cross-sectional power* at a given beam location, s, and over a period T, defined as

$$I_T(s) := \frac{1}{T}\int_0^T \mathbf{x}_1(s,t)^\top \mathbf{x}_2(s,t)\,\mathrm{d}t, \quad s\in[0,S], \;\; T\geq 0, \tag{58}$$

where $\mathbf{x}_1, \mathbf{x}_2$ are, as before, the local inertial velocities and stress resultants, respectively, satisfying Eq. (1) with boundary conditions satisfying Eq. (7). To obtain the invariance property, we first differentiate I_T with respect to arc length s, as

$$\begin{aligned}\frac{\mathrm{d}I_T}{\mathrm{d}s} = \frac{1}{T}\int_0^T [\mathbf{x}_1^\top \mathbf{x}_2{}' + \mathbf{x}_2^\top \mathbf{x}'_1]\,\mathrm{d}t = \frac{1}{T}\int_0^T \mathbf{x}_1^\top(\mathbf{M}\dot{\mathbf{x}}_1 - \mathbf{E}\mathbf{x}_2 + \mathcal{L}(\mathbf{x}_1)\mathbf{M}\mathbf{x}_1 + \mathcal{L}_2(\mathbf{x}_2)\mathbf{C}\mathbf{x}_2 - \mathbf{f}_1)\,\mathrm{d}t \\ + \frac{1}{T}\int_0^T \mathbf{x}_2^\top(\mathbf{C}\dot{\mathbf{x}}_2 + \mathbf{E}^\top \mathbf{x}_1 - \mathcal{L}^\top(\mathbf{x}_1)\mathbf{C}\mathbf{x}_2)\,\mathrm{d}t.\end{aligned} \tag{59}$$

From the definitions of $\mathcal{L}_1$ and $\mathcal{L}_2$ in Eq. (4), it can be seen that $\mathbf{x}_1^\top \mathcal{L}_1(\mathbf{x}_1)\mathbf{M}x_1 = 0$, and $\mathbf{x}_2^\top \mathcal{L}_1^\top(\mathbf{x}_1)\mathbf{C}\mathbf{x}_2 = \mathbf{x}_1^\top \mathcal{L}_2(\mathbf{x}_2)\mathbf{C}\mathbf{x}_2$. As a result, and using the symmetry of $\mathbf{M}$ and $\mathbf{C}$, Eq. (59) can be written as

$$\frac{\mathrm{d}I_T}{\mathrm{d}s} + \frac{1}{T}\int_0^T \mathbf{x}_1^\top \mathbf{f}_1\,\mathrm{d}t = \frac{1}{T}\int_0^T \mathbf{x}_1^\top \mathbf{M}\dot{\mathbf{x}}_1 + \mathbf{x}_2^\top \mathbf{C}\dot{\mathbf{x}}_2\,\mathrm{d}t = \frac{1}{T}\int_0^T \frac{\mathrm{d}}{\mathrm{d}t}\left[\frac{1}{2}\mathbf{x}_1^\top \mathbf{M}\mathbf{x}_1 + \frac{1}{2}\mathbf{x}_2^\top \mathbf{C}\mathbf{x}_2\right]\mathrm{d}t, \tag{60}$$

or

$$\begin{aligned}\frac{\mathrm{d}I_T}{\mathrm{d}s} = \frac{1}{2T}(\mathbf{x}_1(s,T)^\top \mathbf{M}\mathbf{x}_1(s,T) + \mathbf{x}_2(s,T)^\top \mathbf{C}\mathbf{x}_2(s,T)) - \frac{1}{2T}(\mathbf{x}_1(s,0)^\top \mathbf{M}\mathbf{x}_1(s,0) + \mathbf{x}_2(s,0)^\top \mathbf{C}\mathbf{x}_2(s,0)) \\ - \frac{1}{T}\int_0^T \mathbf{x}_1(s,t)^\top \mathbf{f}_1(s,t)\,\mathrm{d}t.\end{aligned} \tag{61}$$

Hence, if $\mathbf{x}_1$ and $\mathbf{x}_2$ are periodic in time with periods T_1 and T_2, respectively, then $I_{\tilde{T}}{}'(s) = 0$ for $\tilde{T} = \mathrm{lcm}(T_1, T_2)$ at any point in which there are no applied forces, i.e., $\mathbf{f}_1(s,t) = 0$ and $t\in[0,\tilde{T}]$. Therefore, points of zero applied force are critical points of the average cross-sectional power $I_{\tilde{T}}(s) = 0$. Furthermore, if there are no applied forces (i.e., the beam is vibrating freely), the natural boundary conditions (7) imply that $I_{\tilde{T}}(0) = I_{\tilde{T}}(S) = 0$ giving $I_{\tilde{T}}(s) = 0$, for each $s\in[0,S]$. This situation corresponds to a nonlinear normal mode (NNM) of the structure [21], and the condition $I_{\tilde{T}}(s) = 0$, for each $s\in[0,S]$, defines then an additional criteria to search for NNMs in 1D structures. This will be exemplified in Section 7.2 in the nonlinear oscillations of an isotropic cantilever beam.

If the solutions $\mathbf{x}_1, \mathbf{x}_2$ are not periodic, but nevertheless satisfy $\mathbf{x}_1, \mathbf{x}_2 \in L^\infty([0,S]\times\mathbb{R}_+)$, then it is easy to see that $\lim_{T\to\infty} I'_T(s) = 0$ for each $s\in[0,S]$ where there are no applied external forces. Again, the spatial boundary conditions imply that, for free vibrations, $\lim_{T\to\infty} I_T(s) = 0$ for each $s\in[0,S]$.

7. Numerical examples

The static equilibrium conditions are obtained from the steady state of the full dynamic equations (1) with constant forces and large added dissipation. The numerical implementation is based on a second-order central difference in space and forward difference in time for static equilibrium computation. A fourth-order Runge–Kutta time-marching algorithm was used to solve the modal equations (20). Although the RK4 numerical scheme is not inherently energy-preserving, results in this section are solved with an automatic selection of timestep (using a relative error tolerance of 0.1 percent) to guarantee that negligible integration errors, as shown in the validation tests.

Two test cases are considered: The first test case (Test-case 1) is an initially straight cantilever with various applied initial velocities and loading distributions, designed to test the convergence of the numerical scheme and the conservation in time of the total energy, $\mathcal{E}$. Test-case 2 is a highly flexible cantilever tested by Pai [29]. Its properties were already used in a previous work [11] to identify nonlinear normal modes (NNMs) and will serve here to study the spatial conservation laws.

7.1. Test-case 1: quantities conserved with time

This is an initially straight cantilever beam with dimensions $50\times 1\times 0.5$ m, mass density 8000 kg/m^3, Young's modulus 200 GPa, and Poisson's ratio 0.3, which is modelled under Euler–Bernoulli assumptions with non-neglibible rotational inertia, that is, $\mathbf{C} = \mathrm{diag}(1/EA, 0, 0, 1/GJ, 1/EI_2, 1/EI_3)$ and $\mathbf{M} = \mathrm{diag}(\rho A, \rho A, \rho A, \rho I_1, \rho I_2, \rho I_3)$.

Our implementation of the geometrically nonlinear beam model in intrinsic modal coordinates is first verified against a standard FEM solution (200 1D 2-noded beam elements simulated with a timestep of 0.02 s in ABAQUS). The initial conditions are a parabolic velocity distribution of the form $v_y(s) = v_z(s) = v_{\max}\cdot(s/S)^2$, with $v_{\max} = 30$ m/s, where y and z are

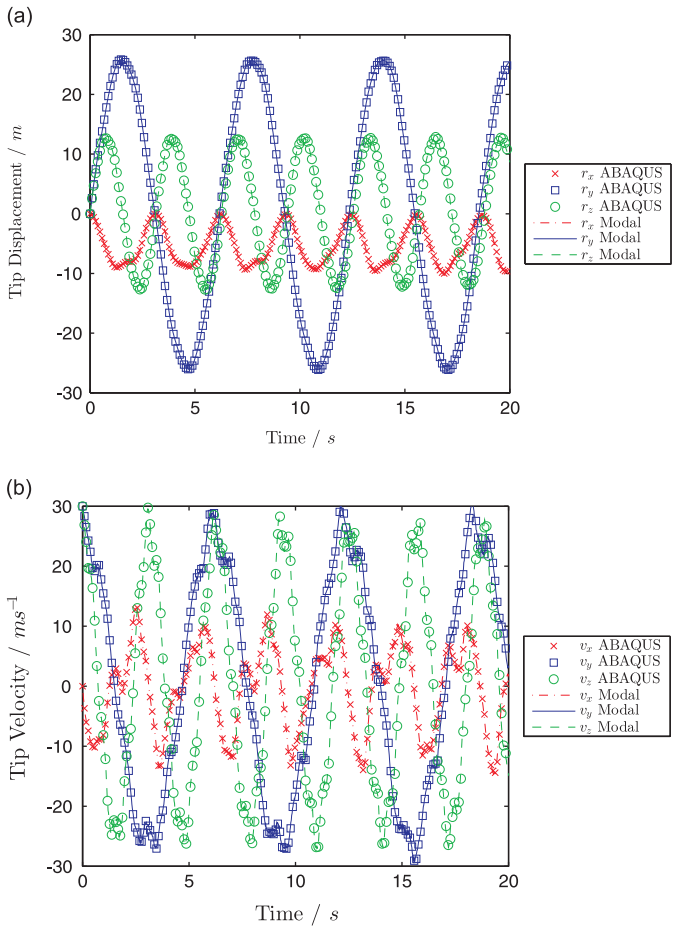

Fig. 1. Displacements (a) and velocities (b) at the free end obtained by the intrinsic model (N=72) and ABAQUS (200 elements, $\Delta t = 0.02$ s). Free vibrations of Test-case 1 with initial parabolic velocity distribution with $v_{max} = 30$ m/s.

in-plane and out-of-plane bending directions, respectively. The beam is then allowed to vibrate freely. Fig. 1 shows the three components, in the inertial coordinate system, of the instantaneous displacement and velocity vectors at the free end. They were obtained using the 72 lowest-frequency modes in the intrinsic model and are compared to the FEM results. It should be noted that in the FEM solution, the displacements are the nodal degrees of freedom, while in the present method they are obtained in two steps: first the local translational and angular velocities are reconstructed from the time-histories of the modal amplitudes, and then they are integrated (using the propagation equations of rigid body dynamics) to determine the instantaneous position and orientation of that particular beam section.

Fig. 2 shows the RMS error in the three components of the tip displacement vector, normalized by the beam length, between the converged results and those obtained with a smaller number of modes. It can be seen that the first 45 modes in the intrinsic description already provide a very good approximation to the FEM results. Note however that no effort was done in those results at removing mode shapes that have a negligible impact in the beam dynamics. For instance, it is clear from Fig. 2 that including modes 21–25 (which are higher-order bending modes) does not result in a significant increase of model accuracy.

In order to demonstrate conservation of total energy, $\mathcal{E}_0(\mathbf{x}_1, \mathbf{x}_2)$, in the unforced oscillations about an undeformed equilibrium, the beam in Test-case 1 is subjected to an initial transverse follower force of 1 MN applied at the free end in the transverse direction (along the local z-axis). This force causes a tip displacement of 32.3 m transversely and 15.74 m longitudinally. The force is then removed, causing the beam to vibrate around its undeformed configuration. The time-marching simulations were obtained in modal coordinates, with modes obtained about $\mathbf{x}_2 = 0$, and using enough modes (N=45) to guarantee convergence. Total system energy $\mathcal{E}_0(\mathbf{x}_1, \mathbf{x}_2)$ is conserved, as can be observed in Fig. 3, which also includes the instantaneous total potential and kinetic energy of the system.

It is more interesting to look at the energy of non-converged finite-dimensional approximations. First, recall that upon expanding modes around the undeformed configuration ($\overline{\mathbf{x}}_2 = 0$), the total ODE energy $\mathcal{E}_0^N(\mathbf{q}_1, \mathbf{q}_2)$ of the $2N$-dimensional approximation is conserved. This was shown analytically in Eq. (33). An illustration of this is presented for the case of N=1

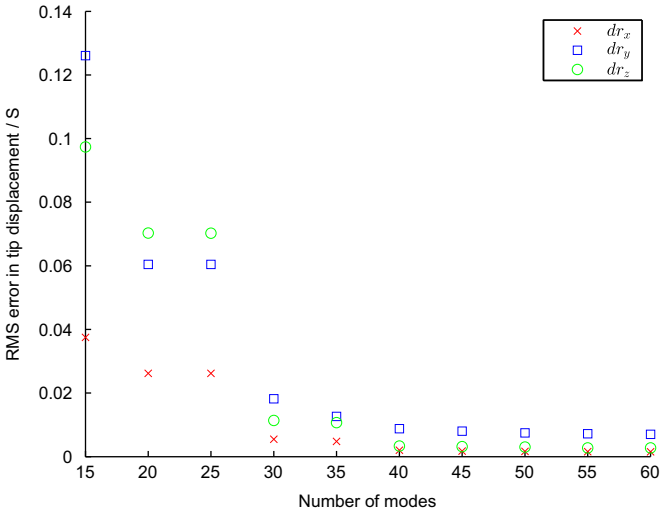

Fig. 2. Average error in the tip displacement with respect to converged ABAQUS simulation. Test-case 1, subject to an initial parabolic velocity distribution with $\mathbf{v}_{\max} = 30$ m/s.

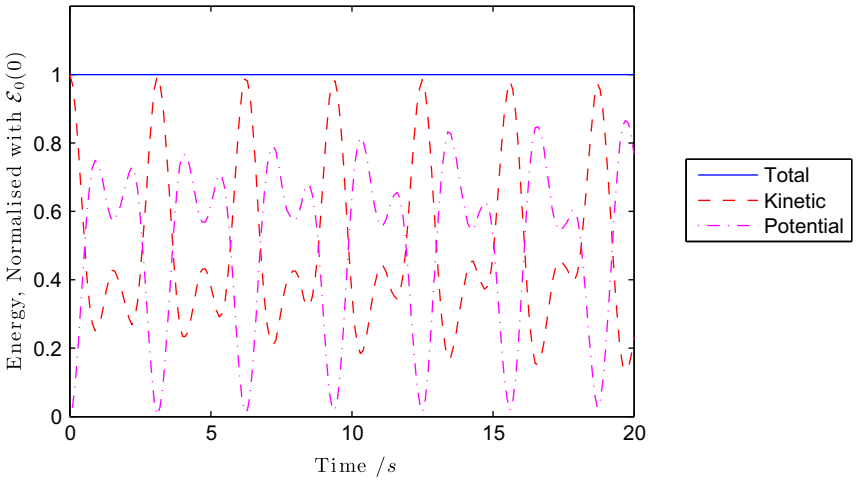

Fig. 3. Total, kinetic and potential energy components. Test-case 1, free vibrations with initial static transverse follower tip load of 1 MN.

and $N=15$ in Fig. 4. Note that mode shapes satisfying the undeformed linearized equations (12), i.e., with $\overline{\mathbf{x}}_2 = 0$, ensure energy conservation in each finite-dimensional approximating system. Note that the energy level in both cases is below 1. This is because the initial conditions were approximated on the modal projection.

Suppose that we instead approximate the nonlinear beam vibrations using modes shapes calculated in terms of the initial (deformed) equilibrium condition, i.e., mode shapes which satisfy (12) for the static loading condition $\overline{\mathbf{x}}_2 \neq 0$. Those results are also included in Fig. 4, for $N \in \{15, 20, 25, 30, 45\}$ and show that the energy is no longer conserved by the finite-dimensional approximations to the full system. However, since the *total energy* of the full system, $\mathcal{E}_0$, given by (22), is conserved, the fluctuations of the finite-dimensional system decrease as more modes are used and the approximation to the full system becomes more accurate. Lastly it can be seen in Fig. 4 that approximately 45 modes are required to observe near energy invariance.

It should be also noted that the initial equilibrium, $\overline{\mathbf{x}}_2$, is not expanded as a modal approximation in the latter case, therefore there is no error in the energy at $t=0$, unlike the case with $\overline{\mathbf{x}}_2 = 0$.

Finally, we consider vibrations about a static, non-zero, equilibrium. In particular, the beam in Test-case 1 is first subject to a transverse follower tipload of 1 MN. Subsequently, an initial parabolic velocity distribution with $v_{\max} = 30$ m/s is again applied and the beam vibrates about the deformed equilibrium $\binom{0}{\overline{\mathbf{x}}_2}$. In this case, neither the total energy $\mathcal{E}_0(\mathbf{x}_1, \mathbf{x}_2)$ nor the perturbation energy $\mathcal{E}_{\overline{\mathbf{x}}_2}(\delta\mathbf{x}_1, \delta\mathbf{x}_2)$ is conserved and the perturbation energy is seen in Fig. 5 to fluctuate with an amplitude of less than 10 percent of $\mathcal{E}_0(\mathbf{x}_1, \mathbf{x}_2)$.

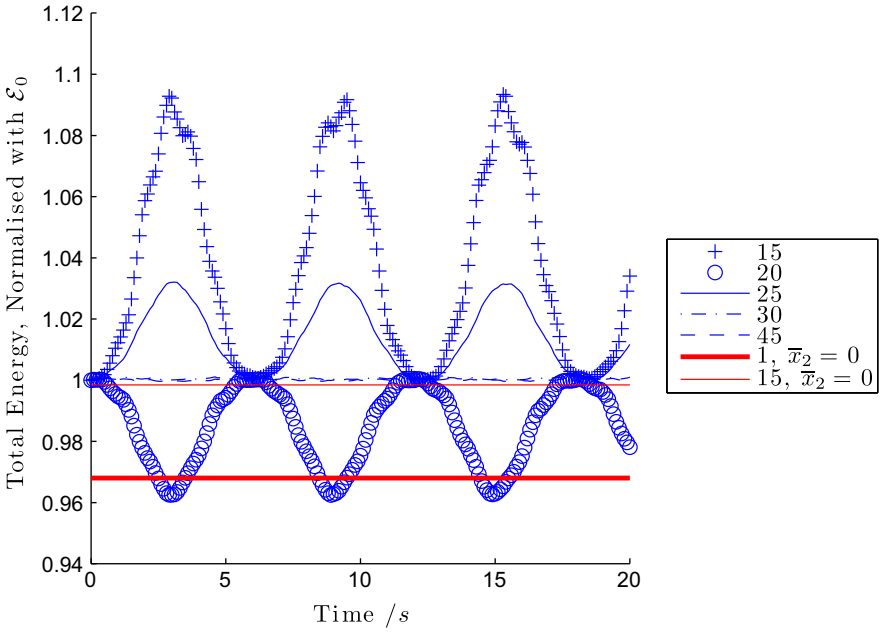

Fig. 4. Total ODE energy $\mathcal{E}_0^N(\mathbf{q}_1, \mathbf{q}_2)$ for approximations with $N \in \{15, 20, 25, 30, 45\}$ modes (around $\overline{\mathbf{x}}_2 \neq 0$) and $N \in \{1, 15\}$ modes (around $\overline{\mathbf{x}}_2 = 0$). Test-case 1, free vibrations with initial static transverse follower tip load of 1 MN.

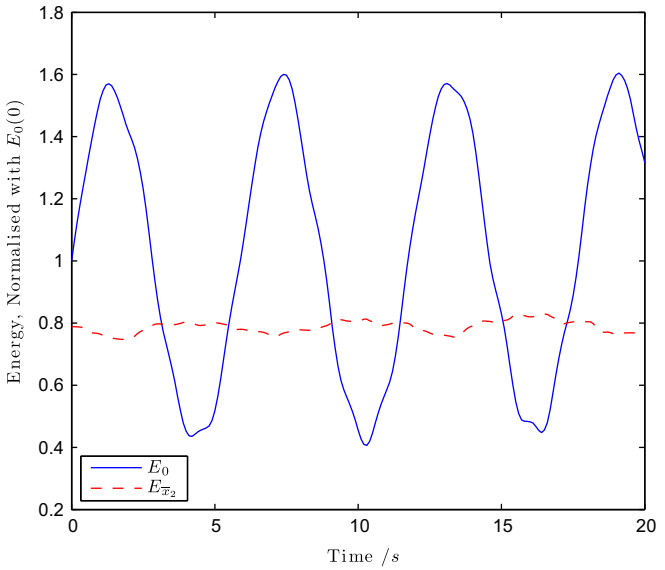

Fig. 5. Variations of $\mathcal{E}_0(\mathbf{x}_1, \mathbf{x}_2)$ and $\mathcal{E}_{\overline{\mathbf{x}}_2}(\delta\mathbf{x}_1, \delta\mathbf{x}_2)$ for an excitation about $\overline{\mathbf{x}}_2 \neq 0$. The beam in Test-case 1 is subject to a static transverse follower tip load of 1 MN. Initial disturbance is the parabolic velocity distribution with $\mathbf{v}_{\max} = 30$ m/s, and the beam subsequently vibrates about $(0\ \overline{\mathbf{x}}_2^{\mathsf{T}})^{\mathsf{T}}$.

To assess the ability of the Casimir approach towards constructing invariant quantities for the forced system dynamics, we consider an ODE approximation of the form (38) to the previous system. This is constructed with $N = 10$ pairs of spatial mode shapes. An initial forcing $\boldsymbol{\eta}_1$ is applied to the ODE system, which corresponds to the 10-mode projection of a transverse follower tip load of 1 MN. The ODE approximation is initialized with a state corresponding to the 10-mode projection of an initial parabolic velocity distribution with $v_{\max} = 30$ m/s. The Lyapunov function $V(\mathbf{q}) = \frac{1}{2}\|\mathbf{q}\|^2 - \boldsymbol{\eta}_1^{\mathsf{T}}\mathcal{C}(\mathbf{q}_2)$ is constructed using the second-order approximation to the Casimir function $\mathcal{C}$, as described in Section 5.2.1. In Fig. 6 the approximation of V is plotted against the total energy $\frac{1}{2}\|\mathbf{q}(t)\|^2$ of the forced system. The Lyapunov function V oscillates at an amplitude of less than 3 percent of that of the total system energy.

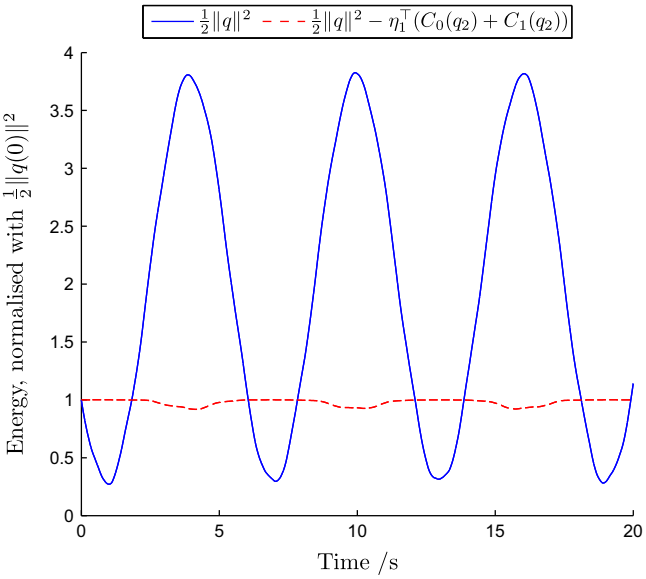

Fig. 6. Total system energy $\mathcal{E}_0^{10}(\mathbf{q}_1, \mathbf{q}_2) = \frac{1}{2}\|\mathbf{q}\|^2$ and the second-order approximation to the Lyapunov function $V(\mathbf{q}) = \frac{1}{2}\|\mathbf{q}\|^2 - \eta_1^\top C(\mathbf{q}_2)$. Quantities calculated using a 10-mode ODE approximation of the beam in Test-case 1. The ODE is subject to a constant forcing η_1 corresponding to the 10-mode projection of a transverse follower tip load of 1 MN. Initial disturbance of the system is the 10-mode projection of a parabolic velocity distribution with $v_{\max} = 30$ m/s.

7.2. Test-case 2: spatially conserved quantities

The second test case uses the configuration tested in Ref. [29], which corresponds to an initially straight very flexible cantilever beam with dimensions $479 \times 50.8 \times 0.45$ mm, mass density 4430 kg/m^3 and Young modulus 127 GPa. It will be used to demonstrate the conservation of the average cross-sectional power I_T, defined in Eq. (58), which was established for periodic beam dynamics. For unforced cases, that state corresponds, by definition, to a NNM and the results of Palacios [11] can be directly used. Here, the initial excitation corresponds to the second NNM of the beam (that is, the NNM that reduces to the second linear bending mode in the zero-energy limit). Two cases are shown in Fig. 7, corresponding to initial velocity amplitude of the second mode of 0.1 and 0.25 (all other modes are defined according to the NNM constraints of Ref. [11]). In Fig. 7 the value of $T \cdot I_T$ is plotted at equally spaced locations from $s = 5$ percent S up to $s = 95$ percent S along the length of the beam. Both simulations show that the integral I_T returns to zero periodically and simultaneously everywhere along the beam. The period of the oscillations changes with the amplitude of vibrations (different energy levels), in accordance with the results in [11]. This change is not very large for the amplitudes under consideration, but it can be seen in the different number of cycles for each of the two cases included in Fig. 7. At the end of each period, the integral $T \cdot I_T$ goes to zero at all locations along the beam, thus demonstrating the conservation of average cross-sectional power.

8. Conclusions

In this paper, conserved quantities are identified in the free vibrations of geometrically nonlinear beams. It is known that the total energy is conserved in time in the free vibrations about an undeformed equilibrium position. More interestingly, if the beam dynamics are approximated using a finite-dimensional ODE model formed using the linear normal modes of an intrinsic description, then the ODE energy is also conserved irrespective of the dimension of the approximating system. This is a remarkable property of the intrinsic form of the beam equations that may offer new insights into nonlinear structural vibrations.

If the beam is subject to a constant forcing, the free vibrations are about a non-zero equilibrium. In this case, the total system energy is in general no longer conserved in the free-vibration phase. However, using Casimir functions, a sufficient condition is derived under which a conserved quantity can be constructed for an ODE approximation of the forced beam dynamics. An additional quantity, identified as the average cross-sectional power, has been shown to be conserved spatially for periodic oscillations of the beam. This has been exemplified for a cantilever beam vibrating in a nonlinear normal mode.

Finally, when time-varying distributed forcing is present, expressions have been given to determine the rate of the change of the corresponding quantities of interest. The properties demonstrated for the finite-dimensional approximations are guaranteed regardless of their actual accuracy in the estimation to the dynamics of the continuous system, which should prove very useful in energy-based methods for nonlinear vibration control.

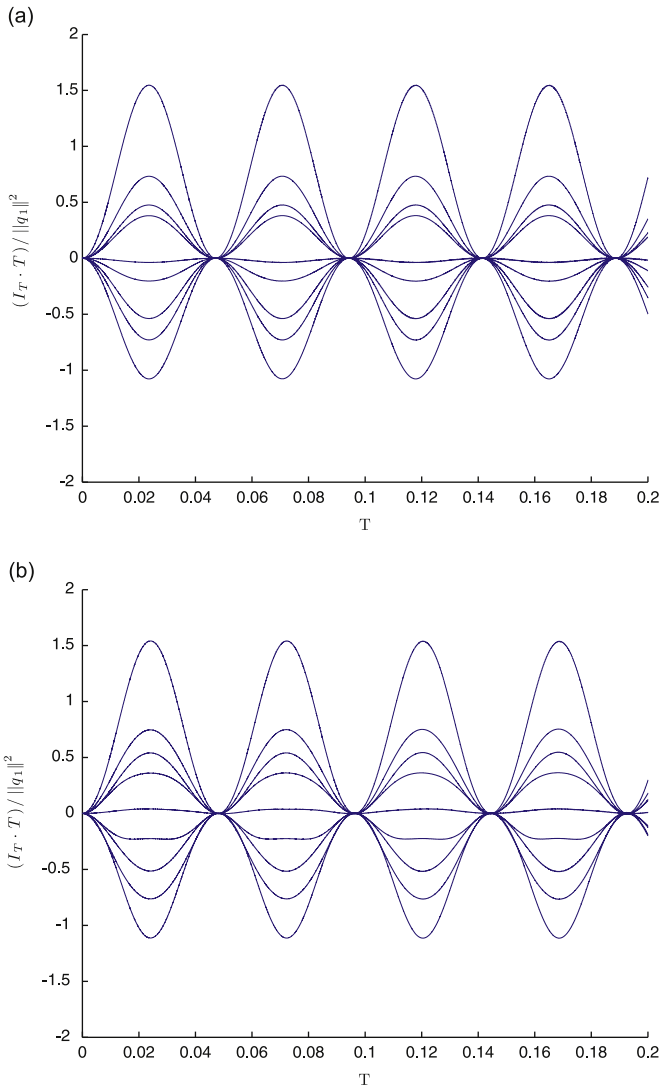

Fig. 7. Normalized value of $T \cdot I_T$ at equally spaced locations along the beam length against the integration time, T, for the second nonlinear normal mode in Test-case 2. Initial conditions are determined by the amplitude in velocities of the second bending mode, $q_{12}(0)$. (a) $q_{12}(0) = 0.1$ (b) $q_{12}(0) = 0.25$.

Acknowledgements

This work is funded by the UK Engineering and Physical Sciences Research Council Grant EP/I014683/1 “Nonlinear Flexibility Effects on Flight Dynamics and Control of Next-Generation Aircraft”.

References

[1] J. Simó, N. Tarnow, K. Wong, Exact energy-momentum conserving algorithms and symplectic schemes for nonlinear dynamics, *Computer Methods in Applied Mechanics and Engineering* 100 (1) (1992) 63–116, http://dx.doi.org/10.1016/0045-7825(92)90115-Z.
[2] J. Simó, N. Tarnow, M. Doblare, Non-linear dynamics of three-dimensional rods—exact energy and momentum conserving algorithms, *International Journal for Numerical Methods in Engineering*, 38 (9) (1995) 1431–1473.
[3] O. Bauchau, C. Bottasso, On the design of energy preserving and decaying schemes for flexible, nonlinear multi-body systems, *Computational Methods in Applied Mechanics and Engineering* 169 (1–2) (1999) 61–79.
[4] M.A. Crisfield, G. Jelenić, Objectivity of strain measures in the geometrically exact three-dimensional beam theory and its finite-element implementation, *Proceedings of the Royal Society of London. Series A: Mathematical, Physical and Engineering Sciences* 455 (1999) 1125–1147.
[5] A. Ibrahimbegovic, S. Mamouri, R. Taylor, A. Chen, Finite element method in dynamics of flexible multibody systems: modeling of holonomic constraints and energy conserving integration schemes, *Multibody System Dynamics* 4 (2/3) (2000) 195–223.
[6] O. Bauchau, *Flexible Multibody Dynamics*, Vol. 176, Springer, 2010.
[7] A. Leung, S. Mao, A symplectic galerkin method for non-linear vibration of beams and plates, *Journal of Sound and Vibration* 183 (3) (1995) 475–491, http://dx.doi.org/10.1006/jsvi.1995.0266.
[8] D. Wagg, S. Neild, *Nonlinear Vibration with Control, Solid Mechanics and its Applications*, Vol. 170, Springer, Dordrecht, The Netherlands, 2010.
[9] A.H. Nayfeh, *Nonlinear Interactions: Analytical, Computational, and Experimental Methods*, John Wiley & Sons, New York, NY, USA, 2000.

[10] K.A. Alhazza, M.F. Daqaq, A.H. Nayfeh, D.J. Inman, Non-linear vibrations of parametrically excited cantilever beamssubjected to non-linear delayed-feedback control, *International Journal of Non-Linear Mechanics* 43 (8) (2008) 801–812, http://dx.doi.org/10.1016/j.ijnonlinmec.2008.04.010.
[11] R. Palacios, Nonlinear normal modes in an intrinsic theory of anisotropic beams, *Journal of Sound and Vibration* 330 (8) (2011) 1772–1792.
[12] G. Hegemier, S. Nair, A nonlinear dynamical theory for heterogeneous, anisotropic, elastic rods, *AIAA Journal* 15 (1) (1977) 8–15.
[13] D. Hodges, Geometrically exact, intrinsic theory for dynamics of curved and twisted anisotropic beams, *AIAA Journal* 41 (6) (2003) 1131–1137.
[14] B. Maschke, R. Ortega, A.J. van der Schaft, Energy-based Lyapunov functions for forced Hamiltonian systems with dissipation, *IEEE Transactions on Automatic Control* 45 (8) (2000) 1498–1502. mechanics and nonlinear control systems.
[15] A. Macchelli, C. Melchiorri, Modeling and control of the Timoshenko beam. The distributed port Hamiltonian approach, *SIAM Journal on Control and Optimization* 43 (2) (2004) 743–767.
[16] C.-S. Chang, D.H. Hodges, M.J. Patil, Flight dynamics of highly flexible aircraft, *Journal of Aircraft* 45 (2) (2008) 538–545.
[17] Z. Sotoudeh, D. Hodges, C.-S. Chang, Validation studies for aeroelastic trim and stability analysis of highly flexible aircraft, *Journal of Aircraft* 47 (4) (2010) 1240–1247.
[18] R. Palacios, B. Epureanu, An intrinsic description of the nonlinear aeroelasticity of very flexible wings, *52nd AIAA/ASME/ASCE/AHS/ASC Structures*, *Structural Dynamics and Materials Conference*, Denver, CO, USA, 2011, aIAA Paper 2011–1917.
[19] Z. Sotoudeh, D.H. Hodges, Modeling beams with various boundary conditions using fully intrinsic equations, *Journal of Applied Mechanics* 78 (3) (2011) 031010.
[20] R. Palacios, Y. Wang, M. Karpel, Intrinsic models for nonlinear flexible-aircraft dynamics using industrial finite-element and loads packages, *53rd AIAA/ASME/ASCE/AHS/ASC Structures*, *Structural Dynamics and Materials Conference*, Honolulu, HI, USA, 2012, AIAA Paper No 2012–1401.
[21] S.W. Shaw, C. Pierre, Normal modes for non-linear vibratory systems, *Journal of Sound and Vibration* 164 (1) (1993) 85–124.
[22] D.H. Hodges, *Nonlinear Composite Beam Theory*, *Progress in Astronautics and Aeronautics*, Vol. 213, AIAA, Reston, VA, USA, 2006.
[23] R. Palacios, J. Murua, R. Cook, Structural and aerodynamic models in the nonlinear flight dynamics of very flexible aircraft, *AIAA Journal* 48 (11) (2010) 2559–2648.
[24] E. Reissner, On one-dimensional large-displacement finite-strain beam theory, *Studies in Applied Mathematics* LII (2) (1973) 87–95.
[25] J.C. Simó, A finite strain beam formulation. the three-dimensional dynamic problem. part i, *Computer Methods in Applied Mechanics and Engineering* 49 (1) (1985) 55–70.
[26] J.L. Kazdan, Perturbation of complete orthonormal sets and eigenfunction expansions, *Proceedings of the American Mathematical Society* 27 (1971) 506–510.
[27] A. Bloch, P. Crouch, J. Bailleiul, J. Marsden, *Nonholonomic Mechanics and Control*, Springer, New York, 2003.
[28] D. Cheng, A. Astolfi, R. Ortega, On feedback equivalence to port controlled Hamiltonian systems, *Systems and Control Letters* 54 (9) (2005) 911–917.
[29] P.F. Pai, *Highly Flexible Structures*: *Modeling, Computation*, *and Experimentation*, AIAA Education Series, American Institute of Aeronautics and Astronautics, Reston, VA, USA, 2007.